

CONF-950104--5

## Simulation and Performance Analysis of a 4-Effect Lithium Bromide-Water Absorption Chiller

### DISCLAIMER

This report was prepared as an account of work sponsored by an agency of the United States Government. Neither the United States Government nor any agency thereof, nor any of their employees, makes any warranty, express or implied, or assumes any legal liability or responsibility for the accuracy, completeness, or usefulness of any information, apparatus, product, or process disclosed, or represents that its use would not infringe privately owned rights. Reference herein to any specific commercial product, process, or service by trade name, trademark, manufacturer, or otherwise does not necessarily constitute or imply its endorsement, recommendation, or favoring by the United States Government or any agency thereof. The views and opinions of authors expressed herein do not necessarily state or reflect those of the United States Government or any agency thereof.

G. Grossman\*  
R. C. DeVault

*A. Zaltash (per Paulette Bunn)*

\*Technion-Israel Institute of Technology

submitted to  
ASHRAE Symposium  
Chicago, Illinois  
January 28 - February 1, 1995

Prepared by the  
OAK RIDGE NATIONAL LABORATORY  
managed by  
MARTIN MARIETTA ENERGY SYSTEMS, INC.  
Oak Ridge, Tennessee 37831-2008  
for the  
U.S. DEPARTMENT OF ENERGY  
under Contract No. DE-AC05-84OR21400

MASTER

"The submitted manuscript has been authored by a contractor of the U.S. government under Contract No. DE-AC05-84OR21400. Accordingly, the U.S. Government retains a nonexclusive, royalty-free license to publish or reproduce the published form of this contribution, or allow others to do so, for U.S. Government purposes."

*LEW ds*  
DISTRIBUTION OF THIS DOCUMENT IS UNLIMITED

## **DISCLAIMER**

**Portions of this document may be illegible in electronic image products. Images are produced from the best available original document.**

## PAPER COVER SHEET

### Simulation and Performance Analysis of a 4-Effect Lithium Bromide-Water Absorption Chiller

by

G. Grossman, Sc.D., ASHRAE Member; A. Zaltash, Ph.D.; and R.C. DeVault

G. Grossman is Professor, Faculty of Mechanical Engineering, Technion-Israel Institute of Technology, Haifa 32000, Israel;

A. Zaltash is Development Staff Member, Energy Division, Oak Ridge National Laboratory, Oak Ridge, Tennessee 37831, USA;

R.C. DeVault is Research Staff Member, Energy Division, Oak Ridge National Laboratory, Oak Ridge, Tennessee 37831, USA.

### ABSTRACT

Performance simulation has been conducted for a 4-effect lithium bromide-water chiller, capable of substantial performance improvement over state-of-the-art double-effect cycles. The system investigated includes four condensers and four desorbers coupled together, forming an extension of the conventional double-effect cycle; based on prior analytical studies, a parallel flow system was preferred over series flow, and double-condenser coupling was employed, to further improve performance. A modular computer code for simulation of absorption systems (ABSIM) was used to investigate the performances of the cycle. The simulation was carried out to investigate the influence of some major design parameters. A coefficient of performance around 2.0 (cooling) was calculated at the design point, with a heat supply temperature of 600°F (315°C) at the solution outlet from the high temperature desorber. With some optimization of the weak (pumped) solution flowrate and of the solution split among the four desorbers, this COP may be raised above 2.2.

Key Words: Absorption, Heat Pump, Chiller, Gas-Fired, Simulation

# Simulation and Performance Analysis of a 4-Effect Lithium Bromide-Water Absorption Chiller

## ABSTRACT

Performance simulation has been conducted for a 4-effect lithium bromide-water chiller, capable of substantial performance improvement over state-of-the-art double-effect cycles. The system investigated includes four condensers and four desorbers coupled together, forming an extension of the conventional double-effect cycle; based on prior experience, a parallel flow system was preferred over series flow, and Double-Condenser Coupling (DCC) was employed, extending from triple-effect cycles, to further improve performance. A modular computer code for simulation of absorption systems (ABSIM) was used to investigate the performances of the cycle. The simulation was carried out to investigate the influence of some major design parameters. A coefficient of performance around 2.0 (cooling) was calculated at the design point, with a heat supply temperature of 600°F (315°C) at the solution outlet from the high temperature desorber. With some optimization of the weak (pumped) solution flowrate and of the solution split among the four desorbers, this COP may be raised above 2.2.

## INTRODUCTION

All current gas-fired residential absorption cooling systems are based on the well-known single-effect or double-effect cycles. Single effect systems ( $COP \approx 0.7$ ) are severely limited in their ability to utilize high temperature heat sources, and are particularly suitable for waste heat or solar applications. The double-effect cycle ( $COP \approx 1.2$ ) represents a significant step in performance improvement over the basic single-effect cycle.

In order to further improve utilization of the high temperature heat available from natural gas, a variety of triple-effect cycles have been proposed, capable of substantial performance improvement over equivalent double-effect cycles. In a recent study (Grossman et al., 1994), several of these cycles were simulated and analyzed in detail. Among the cycles considered were (1) the three-condenser-three-desorber (3C3D) triple-effect cycle (Oouchi et al., 1985), forming an extension of the conventional double-effect cycle, comprising one evaporator, one absorber, three condensers and three desorbers, recovering heat from each high temperature condenser to the next lower temperature desorber; (2) a variation of the 3C3D cycle with Double- Condenser Coupling (DCC) (Miyoshi et al., 1985; DeVault and Biermann, 1993; DeVault and Grossman, 1992) where heat is recovered from the hot condensate leaving the high temperature condensers and added to the lower temperature desorbers; and (3) the dual loop triple-effect cycle (DeVault, 1988) comprising two complete single-effect loops, recovering heat from the condenser and absorber of one loop to the desorber of the other loop and generating a cooling effect in the evaporators of both loops. Other triple-effect configurations are also theoretically possible (Alefeld, 1985; Ziegler and Alefeld, 1994). Important considerations

in comparing the various systems include not only the energy efficiency of the cycle but also its practicality and potential initial cost.

The purpose of the present study has been to investigate the possibility of further improving utilization of the high temperature heat available from natural gas combustion. Performance simulation is conducted for a 4-effect lithium bromide-water cycle including four condensers and four desorbers coupled together, forming an extension of the conventional double-effect cycle. Based on prior experience, a parallel flow system is used in preference over series flow, and Double-Condenser Coupling (DCC) is employed, extending from triple-effect cycles, to further improve performance. One goal of the study is to investigate the effect of various design parameters on the cycle's performance. Some parametric analysis is conducted which indicates performance trends.

## DESCRIPTION OF THE 4-EFFECT CYCLE

Figure 1 describes schematically the 4-effect lithium bromide-water chiller under investigation. The system comprises an evaporator, an absorber, and four pairs of desorbers/condensers coupled together for internal heat recovery. The cycle forms an extension of the conventional double-effect cycle, or of the three-condenser-three-desorber (3C3D) triple-effect cycle (Grossman et al., 1994). The system has 24 components or sub-units (indicated by the circled numbers) and 62 state points (indicated by the uncircled numbers). Absorber (2) and condenser (5) are externally cooled; desorber (22) is externally heated. Chilled water is produced in evaporator (1). Heat rejected from condenser (6) powers desorber (3), heat from condenser (14) powers desorber (4) and heat from condenser (23) powers desorber (13). The coupling between each condenser-desorber pair is through a circulating heat transfer fluid loop, as shown, but may also be achieved by physically combining the two components, such that the refrigerant condensing on one side of a heat exchange surface would heat up the solution desorbing on the other side of that surface. The absorbent solution is in parallel flow, where the weak (weak in LiBr concentration) solution from the absorber is split and divided among the four desorbers. According to simulation results of double-effect cycles (Gommed and Grossman, 1990) and triple-effect cycles (Grossman et al., 1994), the parallel flow arrangement is superior in performance to the series flow in terms of increased COP and a lower risk of crystallization. The condensate leaving the condensers (6),(14) and (23) is mixed with the superheated vapor leaving the desorbers (3),(4) and (13), respectively before proceeding from each to the next lower-temperature condenser. This method, known as Double-Condenser Coupling (DCC) (DeVault and Biermann, 1993) helps subcool each condensate stream and reject the heat to a corresponding desorber. It was shown in an earlier study of triple-effect cycles (Grossman et al., 1994), that the main effect of this heat recuperation is in providing extra cooling capacity to the evaporator through the now subcooled refrigerant, at no additional expenditure of high grade heat. An added benefit is a somewhat increased generation capacity of the desorbers (3) and (4).

## METHODOLOGY OF SIMULATION

A modular computer code for simulation of absorption systems (ABSIM) was used to investigate the performance of the cycle under study. The code, developed specifically for flexible cycle simulation, has been described in detail by Grossman and Wilk (1992) and in a related report (Grossman et al., 1991) containing a user's manual. The modular structure of the code makes it possible to simulate a variety of absorption systems in varying cycle configurations and with different working fluids. The code is based on unit subroutines containing the governing equations for the system's components and on property subroutines containing thermodynamic properties of the working fluids. The components are linked together by a main program which calls the unit subroutines according to the user's specifications to form the complete cycle. When all the equations for the entire cycle have been established, a mathematical solver routine is employed to solve them simultaneously. The code is user-oriented and requires a relatively simple input containing the given operating conditions and the working fluid at each state point. The user conveys to the computer an image of the cycle by specifying the different components and their interconnections. Based on this information, the code calculates the temperature, flowrate, concentration, pressure and vapor fraction at each state point in the system and the heat duty at each unit, from which the coefficient of performance may be determined. The code has been employed successfully to simulate a variety of single-effect, double-effect and dual loop absorption chillers, heat pumps and heat transformers employing the working fluids  $\text{LiBr-H}_2\text{O}$ ,  $\text{H}_2\text{O-NH}_3$ ,  $\text{LiBr/ZnBr}_2\text{-CH}_3\text{OH}$ ,  $\text{NaOH-H}_2\text{O}$  and more. Recently, the same code was used to simulate the rather complex Generator-Absorber Heat Exchange (GAX) cycle employing ammonia-water, in several cycle variations, and a variety of triple-effect chillers employing lithium bromide-water (Grossman et al., 1994).

The simulation methodology in the present study has followed an approach taken in earlier studies of single- and double-effect cycles (Gommed and Grossman, 1990), and triple-effect cycles (Grossman et al., 1994). Since the performance of each system depends on many parameters, the approach has been to establish a design point for the system, and vary the relevant parameters around it. In particular, a performance map of COP and cooling capacity as functions of desorber heat supply temperature was generated for each system. Thus, the performance of systems in single, double and triple stages could be compared not only at a single point but over the entire temperature domain applicable to the cycle.

The system's performance under a given set of operating conditions depends, of course, on the design characteristics and particularly on the size of the heat transfer surfaces in its exchange units — the evaporators, absorbers, condensers and desorbers. As a reference case, a practical system was considered with economically reasonable, if not optimized, heat transfer areas. In the earlier study of simpler systems (Gommed and Grossman, 1990) a single-effect solar-powered lithium bromide-water chiller known as SAM-15 (Biermann, 1978) was selected as a reference case. SAM-15 has been tested extensively. An extension of this study to triple-effect systems (Grossman et al., 1994) has employed the same approach. Here, a reference case have been created for a 4-effect

lithium bromide-water chiller according to Figure 1, with SAM-15 size (specified in terms of its UA) of the evaporator, absorber, condensers, desorbers and heat exchangers (recuperators), and with SAM-15 flows of the external fluids. Selecting the reference case in this manner made it possible to use the results of the present simulation for comparison with those of the simpler, single-, double- and triple-effect cycles (Gommed and Grossman, 1990; Grossman et al., 1994), on an equivalent basis. The design characteristics of the 4-effect reference system are listed in Table 1, including the externally imposed flowrates of cooling and chilled water; the weak absorbent circulation rate; the UA's (overall heat transfer coefficient times area), which characterize the heat transfer performance of the exchange units; and design point temperatures of the external fluids and of the solution outlet from the gas-fired desorber (for this desorber, unit 22, the external fluid loop is redundant). With these values as input, the simulation code calculates the internal temperatures, flowrates, concentrations, and other operating parameters at all the system's state points from which overall performance parameters may be derived.

Unfortunately, measured property data for lithium bromide-water are not available in the literature at temperatures beyond 210°C (410°F). Properties of lithium bromide-water for the simulation were taken from the ASHRAE Handbook (1985) and extrapolated, where necessary, to the high temperature range required by the 4-effect cycle. The extrapolation was done by employing the same correlations given in the ASHRAE Handbook (1985) at the high temperatures, beyond their stated range of validity. A comparison of the properties thus obtained was carried out later with the higher-temperature LiBr-water data developed recently under the ASHRAE Research Program (Jeter et al., 1992; Lenard et al., 1992), which are valid up to 210°C (410°F). The differences in vapor pressures and specific heat were on the order of a few percents, and hence the extrapolations were considered adequate for a first evaluation of the 4-effect cycle. A more detailed evaluation leading to actual design will have to rely on more accurate property data that may become available in the future.

## RESULTS OF SIMULATION

In conducting the simulation to generate the operating curves of the 4-effect system, the solution outlet temperature from the gas-fired desorber (22) (state point 57) was varied while all the other design parameters were kept constant. For the exchange units, it was assumed that the values of the UA's remain constant while the temperatures and all the other unspecified parameters change. In reality, this is not strictly accurate; although the heat transfer areas (A) remain constant, the heat transfer coefficients (U) vary somewhat with the temperatures as well as with the loading conditions. However, this variation is relatively small in most cases and the assumption of constant UA is a reasonably good approximation. Better fundamental understanding of the combined heat and mass transfer process in absorption and desorption would allow taking the variation of UA with temperature into consideration.

The coefficient of performance (COP) has been defined here as the ratio of the heat

quantity in the evaporator producing the desired cooling effect, to that supplied to the externally heated high temperature desorber. The effect of pumping and other parasitic losses is not considered.

Figure 2 describes the COP of the 4-effect cycle as a function of the heat supply temperature to the externally heated desorber (22), for different cooling water inlet temperatures, and for a fixed chilled water outlet temperature. The weak solution split among the four desorbers remains even. COP curves for the equivalent double- and triple-effect, DCC parallel-flow systems with SAM-15 size components (specified in terms of their UA's, per Table 1), are plotted along for comparison. It is evident that all systems exhibit the same typical, qualitative behavior, with the COP increasing sharply from zero at some minimum temperature, then levelling off to some constant value at a higher temperature and even decreasing slightly with further increase in temperature. The reason for this behavior is well understood and is explained in detail in the above reference (Gommed and Grossman, 1990). The 4-effect system has a COP higher than the double- and triple-effect cycles but requires a higher minimum heat supply temperature in order to begin operating. Figure 2 indicates that the double-effect system performs best at the heat supply temperature range of 300-350°F (150-180°C). Above that, from the COP point of view, it is beneficial to switch to the triple-effect system, which performs best at the heat supply temperature range of 400-450°F (200-230°C). With a still higher heat supply temperature, a 4-effect system is more desirable.

Figure 3 describes the cooling capacity of the 4-effect cycle as a function of the heat supply temperature to the externally heated desorber (22), for different cooling water inlet temperatures, and for a fixed chilled water outlet temperature. The curves for the equivalent double- and triple-effect, DCC parallel-flow systems with SAM-15 size components, are plotted along for comparison. It is evident that all systems exhibit the same typical, qualitative behavior, with the capacity increasing almost linearly with the heat supply temperature. For each system, the lower the cooling water temperature, the higher the capacity. Note that unlike the COP which increases with the number of effects, the capacity is highest for the double-effect system and lowest for the 4-effect system for the same temperature. This is a direct result of the way the three systems were created, with SAM-15 size components, for comparison to each other. The same total amount of weak solution is distributed more thinly among more desorbers, the higher the number of effects, thus producing less refrigerant out of each desorber. Under these conditions, a lower capacity is the price one must pay for the higher COP. However, there is ample room for optimization of the solution flowrates and of the heat transfer area among the system's components to improve upon the capacity or the COP, as will be shown next.

The solution flowrate distribution among the four desorbers in the 4-effect system has been selected equal at the design point. However, an equal distribution of solution is not necessarily optimal. Based on the simulation of double-effect systems (Gommed and Grossman, 1990) and triple-effect systems (Grossman et al., 1994), an improvement may be gained by deviating from an equal distribution both in increasing the COP and reducing the risk of crystallization. Here, the effect of varying the solution flowrate to the

four desorbers has been investigated, with the system operating otherwise at the design condition, per Table 1. Table 2 lists the results of several runs with different flow distribution among the four desorbers (units 3, 4, 13 and 22), showing in each case the cooling capacity and the COP. Note that the sum of the four flowrates is kept constant at the design value of 60 lbs/min (27 kg/min). While Table 2 does not cover the entire range of possibilities, it indicates an optimal (maximum COP) distribution of solution to the high-, medium- and low-temperature desorbers of approximately 40, 10, 5 and 5 lbs/min (18, 5, 2 and 2 kg/min), respectively. Under this condition, the COP reaches 2.177, instead of 2.013 at equal distribution; the solution concentration at the absorber inlet (state point 1) is reduced to 59.2 wt% LiBr, compared to 63.5 wt% LiBr at equal distribution. The capacity is reduced somewhat due to the lower concentration, to 2567.7 from 3964.5 Btu/min (45.1 kW from 69.7 kW) at equal distribution. Note that the optimum flow distribution at the design temperatures is not necessarily preserved in off-design conditions. Also, in the extreme cases where either of the four desorbers is starved for solution, the entire system goes out of balance and both the COP and capacity tend to zero.

It is known from earlier work (Gommed and Grossman, 1990) that the flowrate of solution has an important effect on performance and an optimum value, since too large a solution flowrate leads to excessive circulation losses and too little is insufficient to supply the required amount of refrigerant. Figure 4 shows the cooling capacity normalized with respect to the total UA in the system's components ( $Q_{evap.}/UA_{total}$ ) and the cooling COP of the 4-effect system as functions of total weak (pumped) solution flowrate at state point 5. The system operates otherwise at the design condition (Table 1), with equal distribution of the solution among the four desorbers. It is evident that the total solution flowrate yielding maximum COP is approximately 8.0 lbs/min (3.6 kg/min), deviating considerably from the design condition, with a COP of 2.431 and a capacity of 1556 Btu/min (27.3 kW); ( $Q_{evap.}/UA_{total} = 0.40^{\circ}\text{F}$  or  $0.22^{\circ}\text{C}$ ). However, if the cooling capacity is to be maximized, the optimal solution flowrate is approximately 60 lbs/min (27 kg/min) as selected for the design condition, with a COP of 2.013 and a capacity of 3964.5 Btu/min (69.7 kW); ( $Q_{evap.}/UA_{total} = 1.019^{\circ}\text{F}$  or  $0.566^{\circ}\text{C}$ ).

In addition to capacity and COP, the value of  $Q_{evap.}/UA_{total}$  is an interesting performance criterion, making it possible to compare systems of different sizes. The heat exchange size for the components of the 4-effect system may be characterized not only in terms of their UA's, but also using the effectiveness (EFF) or the closest approach temperature (CAT). Figure 5 shows the variation of the cooling COP and  $Q_{evap.}/UA_{total}$  with the effectiveness, assumed the same for all the system's components, units 1-8, 12-14, 21 and 23. The cooling COP increases with increased effectiveness. However,  $Q_{evap.}/UA_{total}$  goes through a maximum at an effectiveness of approximately 0.7. The reason for this maximum is that a high effectiveness yields better performance, but at the same time requires larger UA's, the return for which diminishes at high effectivenesses. Figure 6 describes the effect of the closest approach temperature on the cooling COP and  $Q_{evap.}/UA_{total}$ . It is evident that the COP decreases with increasing CAT, quite substantially with CAT's greater than  $10^{\circ}\text{F}$  ( $5.5^{\circ}\text{C}$ ). The  $Q_{evap.}/UA_{total}$  reaches a maximum approximately at CAT= $7.5^{\circ}\text{F}$  ( $4.2^{\circ}\text{C}$ ) with a COP of 2.231. The results of these runs suggest that the desorbers of the

base case (SAM-15 size) have been oversized and the absorber undersized for the 4-effect cycle.

As mentioned earlier, the system's performance under a given set of operating conditions depends on the design characteristics and particularly on the size of the heat transfer surfaces in its exchange units. As a base case, a practical system was considered with economically reasonable, if not optimized, heat transfer areas. In search of the optimum size of the components, several runs were made with different UA's of the components, presented in Table 3. The results show case #6 to give the best COP, cooling capacity and  $Q_{evap.}/UA_{total}$  among the test cases studied. Performance map of COP and cooling capacity with case #6 UA's as functions of desorber heat supply temperature (Figures 7 and 8) show the significant improvement over the base case. As can be seen, with some optimization of the UA's, the COP was raised above 2.2, with approximately half the heat transfer surface of the base case system's components.

## TECHNICAL OUTLOOK

The results of the present simulation have shown the 4-effect cycle capable of providing a COP increase on the order of 15% over the equivalent triple-effect cycle (Grossman et al., 1994) - 2.013 vs. 1.724, respectively, at the design point. The UA investment relative to the equivalent triple-effect in the base case is an additional 27% (4158 Btu/min. $^{\circ}$ F or 131.8 kW/ $^{\circ}$ C total UA vs. 3261 Btu/min. $^{\circ}$ F or 103.4 kW/ $^{\circ}$ C, respectively). There is still room for optimizing the flow split among the four desorbers, the UA distribution in the system etc. which have not been fully investigated. However, there are several practical considerations which will determine the commercial feasibility of the 4-effect and its capability to replace the triple-effect cycle:

1. Flue losses: The need to provide a higher firing temperature is associated with a lower combustion efficiency due to higher flue gas losses. While some of the exhaust heat may be recovered through an economizer (air preheater), the usefulness of doing this is not clear and must still be determined.
2. Corrosion: A higher corrosion rate is expected at the high temperature components (Desorber 22 and Recuperator 21) which may require more expensive materials of construction and corrosion inhibitors.
3. Heat/mass transfer enhancement additives: The ability of the commonly used additives, such as 2-ethyl-1-hexanol, to survive at the high temperature is very limited. This is also a problem, for that matter, in triple-effect cycles and requires further study.

## CONCLUSION

Performance simulation has been carried out for a lithium bromide-water chiller based on the 4-effect cycle. A reference condition was established based on the component sizes and flowrates of the single-effect SAM-15 system. Performance simulation was carried out over a range of operating conditions, including some investigation of the

influence of the design parameters. A COP of 2.103 was calculated at the design point. The study showed ample room for substantial optimization of the COP, capacity and  $Q_{evap.}/UA_{total}$  by varying the flow and UA distribution among the components with little increase in potential cost.

## ACKNOWLEDGEMENT

This work has been supported in part under Oak Ridge National Laboratory Subcontract 80X-SK033V.

## LIST OF SYMBOLS AND ABBREVIATIONS

CAT	-	Closest Approach Temperature
COP	-	Coefficient of Performance
DCC	-	Double-Condenser Coupling
EFF	-	Heat transfer effectiveness
$Q_{evap.}$	-	Evaporator (cooling) capacity
s.p.	-	State Point
TH	-	Temperature of solution leaving the externally heated, gas-fired desorber, characterizing the heat supply temperature (e.g. $T_{s7}$ in Figure 1)
TC	-	Cooling water supply (inlet) temperature (e.g. $T_3$ and $T_{23}$ in Figure 1)
UA	-	Overall heat transfer coefficient times area
$UA_{total}$	-	Total UA of exchange units (units 1-8, 12-14, 21 and 23 in Figure 1)

## REFERENCES

Alefeld, G., 1985: "Multi-stage apparatus having working fluid and absorption cycles, and method of operation thereof." U.S. Patent 4,531,372, July 30.

ASHRAE Handbook of Fundamentals, 1985 : Thermodynamic Properties of Lithium Bromide-Water. pp. 17.69-17.70.

Biermann, W. J., 1978: "Prototype energy retrieval and solar system, Bonneville Power Administration", *Proceedings, 3rd Workshop on the Use of Solar Energy for Cooling of Buildings*, San Francisco, CA, pp. 29-34. Also personal communication regarding Carrier SAM-15 solar-powered water-lithium bromide absorption chiller, July 1986.

DeVault, R.C. and Biermann, W.J., 1993: "Triple-effect absorption refrigeration system with double-condenser coupling". US Patent 5,205,136.

DeVault, R.C., 1988: "Triple-effect absorption chiller utilizing two refrigerant circuits". US Patent 4,732,008, March 22.

DeVault, R.C. and Grossman, G., 1992: "Triple-effect absorption chiller cycles". Presented at the International Gas Research Conference IGRC92, Orlando, Florida, November 16-19.

Gommed, K. and Grossman, G., 1990: "Performance analysis of staged absorption heat pumps: Water-lithium bromide systems". ASHRAE paper No. AT-90-30-6, presented at the 1990 ASHRAE Winter Meeting, Atlanta, GA, February 10-14.

Grossman, G., Gommed, K. and Gadoth, D., 1991: "A computer model for simulation of absorption systems in flexible and modular form," ORNL/sub/90-89673, Oak Ridge National Laboratory. Also ASHRAE paper No. NT-87-29-2, presented at the ASHRAE Annual Meeting, Nashville, TN, June 27-July 1, 1987.

Grossman, G. and Wilk, M., 1992: "Advanced modular simulation of absorption systems". Presented at the 1992 ASME Winter Annual Meeting, Anaheim, CA, November 8-13.

Grossman, G., Wilk, M. and DeVault, R.C., 1994: "Simulation and performance analysis of triple-effect absorption cycles." Presented at the ASHRAE Winter Meeting, New Orleans, Louisiana, January 22-26.

Jeter, S.M., Moran, J.P. and Teja, A.S., 1992: "Properties of lithium bromide-water solutions at high temperatures and concentrations - Part III: Specific Heat." ASHRAE Transactions, v. 98 pt 1, 137-149.

Lenard, J.L.Y., Jeter, S.M. and Teja, A.S., 1992: "Properties of lithium bromide-water solutions at high temperatures and concentrations - Part IV: vapor pressure." ASHRAE Transactions, v. 98 pt 1, 167-172.

Miyoshi, N., Sugimoto, S. and Aizawa, M., 1985: "Multi-Effect Absorption Refrigerating Machine", US Patent 4,551,991, November 12.

Ouchi, T., Usui, S., Fukuda, T. and Nishiguchi, A., 1985: "Multi-Stage Absorption Refrigeration System". U.S. Patent 4,520,634, June 4.

Ziegler, F. and Alefeld, G., 1994: "Comparison of multi-effect absorption cycles." *Proceedings of the International Absorption Heat Pump Conference*, New Orleans, Louisiana, January 19-21, ASME vol. AES-31.

**TABLE 1**  
**Characteristic Parameters at Design Point for 4-Effect LiBr-H<sub>2</sub>O Absorption Chiller**

Heat Transfer Characteristics (UA):

Absorber:	193.0 Btu/min. °F (6.118 kW/°C)
Desorbers:	268.0 Btu/min. °F (8.496 kW/°C)
Condensers:	565.0 Btu/min. °F (17.911 kW/°C)
Evaporator:	377.0 Btu/min. °F (11.951 kW/°C)
Recuperative Heat Exchangers:	64.0 Btu/min. °F (2.029 kW/°C)

Mass Flow Rates:

Absorber (cooling water)	483.0 lbs/min (219 kg/min)
Low Temperature Condenser (cooling water)	391.0 lbs/min (178 kg/min)
Evaporator (chilled water)	300.0 lbs/min (136 kg/min)
Internal Coupling Water Loops, s.p. 10-11, 15-16 and 35-36	400.0 lbs/min (182 kg/min)
Weak Solution	60.0 lbs/min (27 kg/min)
Solution split evenly among the four desorbers, each	15.0 lbs/min (6.75 kg/min)

Temperatures:

Hot solution outlet from gas-fired desorber (22) (s.p. 57)	600°F (315°C)
Cooling water inlet (s.p. 3 and 23)	85°F (29°C)
Chilled water outlet (s.p. 29)	45°F (7°C)

**TABLE 2**  
**Effect of Solution Distribution Among Desorbers in a**  
**4-Effect LiBr-H<sub>2</sub>O Absorption Chiller at TH = 600°F (315°C)**  
**from lowest to highest temperature generator (left to right),**  
**Conversion factors: kg/min = 0.454 x lbs/min and kW = 0.01757 x Btu/min**

Unit 3 mass flow s.p. 8 (lbs/min)	Unit 4 mass flow s.p. 13 (lbs/min)	Unit 13 mass flow s.p. 33 (lbs/min)	Unit 22 mass flow s.p. 53 (lbs/min)	Q <sub>evap.</sub> (Btu/min)	COP
5	5	15	35	3294.9	1.5578
10	15	15	20	4019.7	1.9250
15	15	15	15	3964.5	2.0131
20	15	15	10	3663.1	2.0750
30	10	10	10	3496.6	2.1374
35	10	7.5	7.5	3129.7	2.1670
40	10	5	5	2567.7	2.1768
45	5	5	5	2419.8	2.1527
35	15	5	5	2600.7	2.1646

**Table 3. Effect of UA distribution among the heat-exchange units in a 4-effect DCC parallel flow system at a fixed total solution flowrate of 60 lbs/min or 27 kg/min (equal distribution) and fixed heat supply temperature of 600°F (315°C), Conversion factors: kW/°C = 0.0317 x Btu/min.°F, kW = 0.01757 x Btu/min and  $\Delta°C = \Delta°F/1.8$**

Unit No.	Unit type	UA base case	UA Case #1	UA Case #2	UA Case #3	UA Case #4	UA Case #5	UA Case #6
1	Evap.	377.0	377.0	377.0	377.0	377.0	377.0	377.0
2	Abs.	193.0	193.0	193.0	100.0	250.0	300.0	400.0
3	Des.	268.0	150.0	100.0	100.0	100.0	100.0	100.0
4	Des.	268.0	150.0	100.0	100.0	100.0	100.0	100.0
5	Cond.	565.0	200.0	100.0	100.0	100.0	100.0	100.0
6	Cond.	565.0	200.0	100.0	100.0	100.0	100.0	100.0
7	HX	64.0	100.0	100.0	100.0	100.0	100.0	100.0
8	HX	64.0	100.0	100.0	100.0	100.0	100.0	100.0
12	HX	64.0	100.0	100.0	100.0	100.0	100.0	100.0
13	Des.	268.0	150.0	100.0	100.0	100.0	100.0	100.0
14	Cond.	565.0	200.0	100.0	100.0	100.0	100.0	100.0
21	HX	64.0	64.0	64.0	64.0	64.0	64.0	64.0
23	Cond.	565.0	200.0	100.0	100.0	100.0	100.0	100.0
Total (Btu/min.°F)		3890.0	2184.0	1634.0	1541.0	1691.0	1741.0	1841.0
COP		2.0130	2.1117	2.0617	1.9212	2.0980	2.1190	2.1460
$Q_{evap.}$ (Btu/min)		3964.5	3733.6	3322.4	2291.9	3715.1	3977.1	4357.1
$Q_{evap.}/UA_{total}$ (°F)		1.02	1.71	2.03	1.49	2.20	2.28	2.37

## LIST OF FIGURES

Figure 1: Schematic description of 4-effect chiller in parallel flow

Figure 2: COP for double-effect, triple-effect, and 4-effect DCC parallel flow LiBr-H<sub>2</sub>O systems as a function of heat supply temperature (TH) for different cooling water temperatures (TC) and a chilled water temperature fixed at 45°F (7.2°C),  
Conversion factor: °C = (°F -32)/1.8

Figure 3: Cooling capacity for double-effect, triple-effect, and 4-effect DCC parallel flow LiBr-H<sub>2</sub>O systems as a function of heat supply temperature (TH) for different cooling water temperatures (TC) and a chilled water temperature fixed at 45°F (7.2°C),  
Conversion factors: °C = (°F -32)/1.8 and kW = 0.01757 x Btu/min

Figure 4: COP and normalized cooling capacity for 4-effect DCC parallel flow LiBr-H<sub>2</sub>O systems as a function of total solution flowrate (equal distribution) at a fixed heat supply temperature (TH) of 600°F (315°C) and fixed UA's,  
Conversion factors: kg/min = 0.454 x lb/min and  $\Delta$ °C =  $\Delta$ °F/1.8

Figure 5: COP and normalized cooling capacity for 4-effect DCC parallel flow LiBr-H<sub>2</sub>O systems as a function of effectiveness (EFF) at a fixed total solution flowrate of 60 lbs/min or 27 kg/min (equal distribution) and fixed heat supply temperature (TH) of 600°F (315°C), Conversion factor:  $\Delta$ °C =  $\Delta$ °F/1.8

Figure 6: COP and normalized cooling capacity for 4-effect DCC parallel flow LiBr-H<sub>2</sub>O systems as a function of closest approach temperature (CAT) at a fixed total solution flowrate of 60 lbs/min or 27 kg/min (equal distribution) and fixed heat supply temperature (TH) of 600°F (315°C), Conversion factor:  $\Delta$ °C =  $\Delta$ °F/1.8

Figure 7: COP for 4-effect base case and 4-effect optimum case (#6 per Table 3) DCC parallel flow LiBr-H<sub>2</sub>O systems as a function of heat supply temperature (TH) for different cooling water temperatures (TC) and a chilled water temperature fixed at 45°F (7.2°C), Conversion factor: °C = (°F -32)/1.8

Figure 8: Cooling capacity for 4-effect base case and 4-effect optimum case (#6 per Table 3) DCC parallel flow LiBr-H<sub>2</sub>O systems as a function of heat supply temperature (TH) for different cooling water temperatures (TC) and a chilled water temperature fixed at 45°F (7.2°C), Conversion factors: °C = (°F -32)/1.8 and kW = 0.01757 x Btu/min

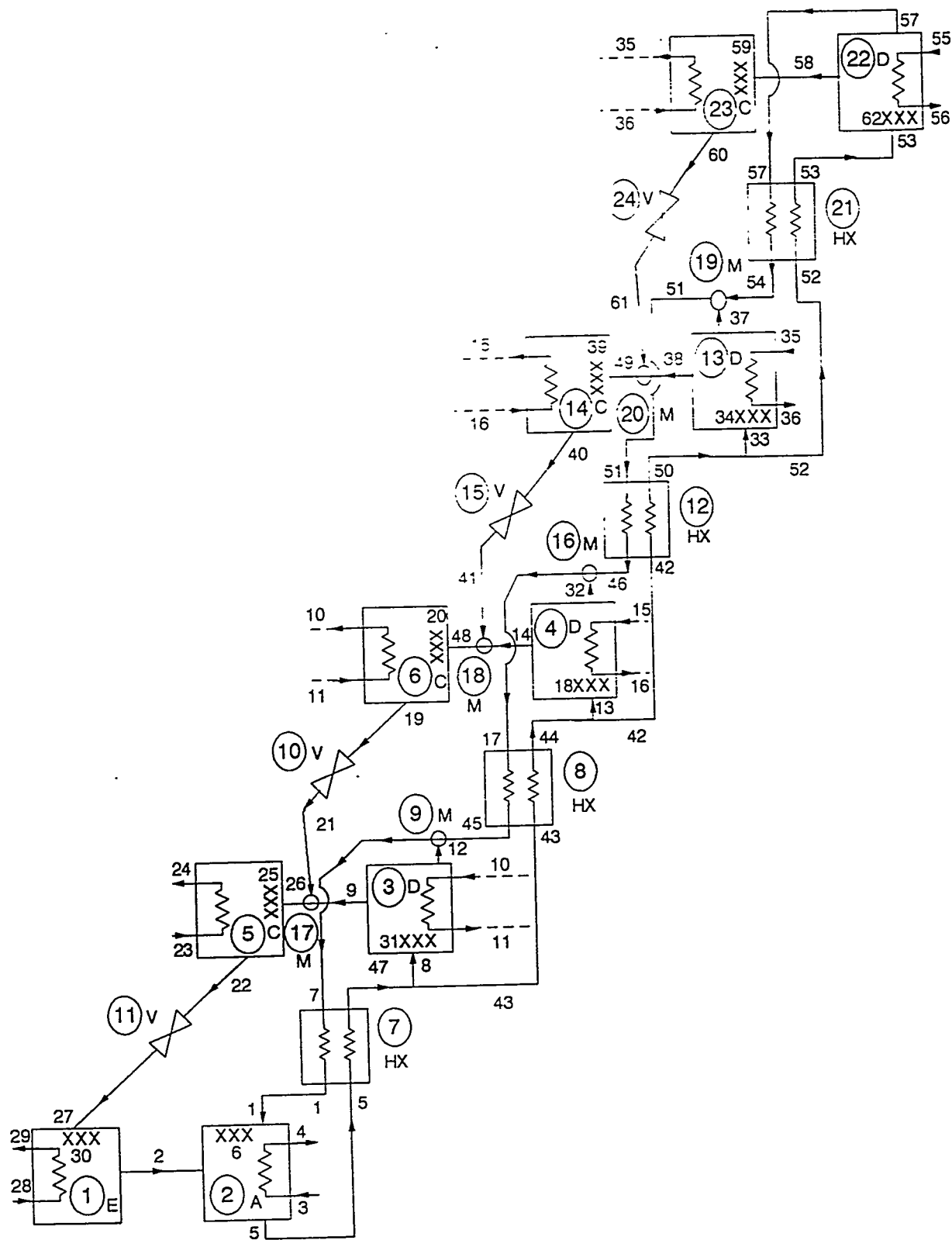


Figure 1

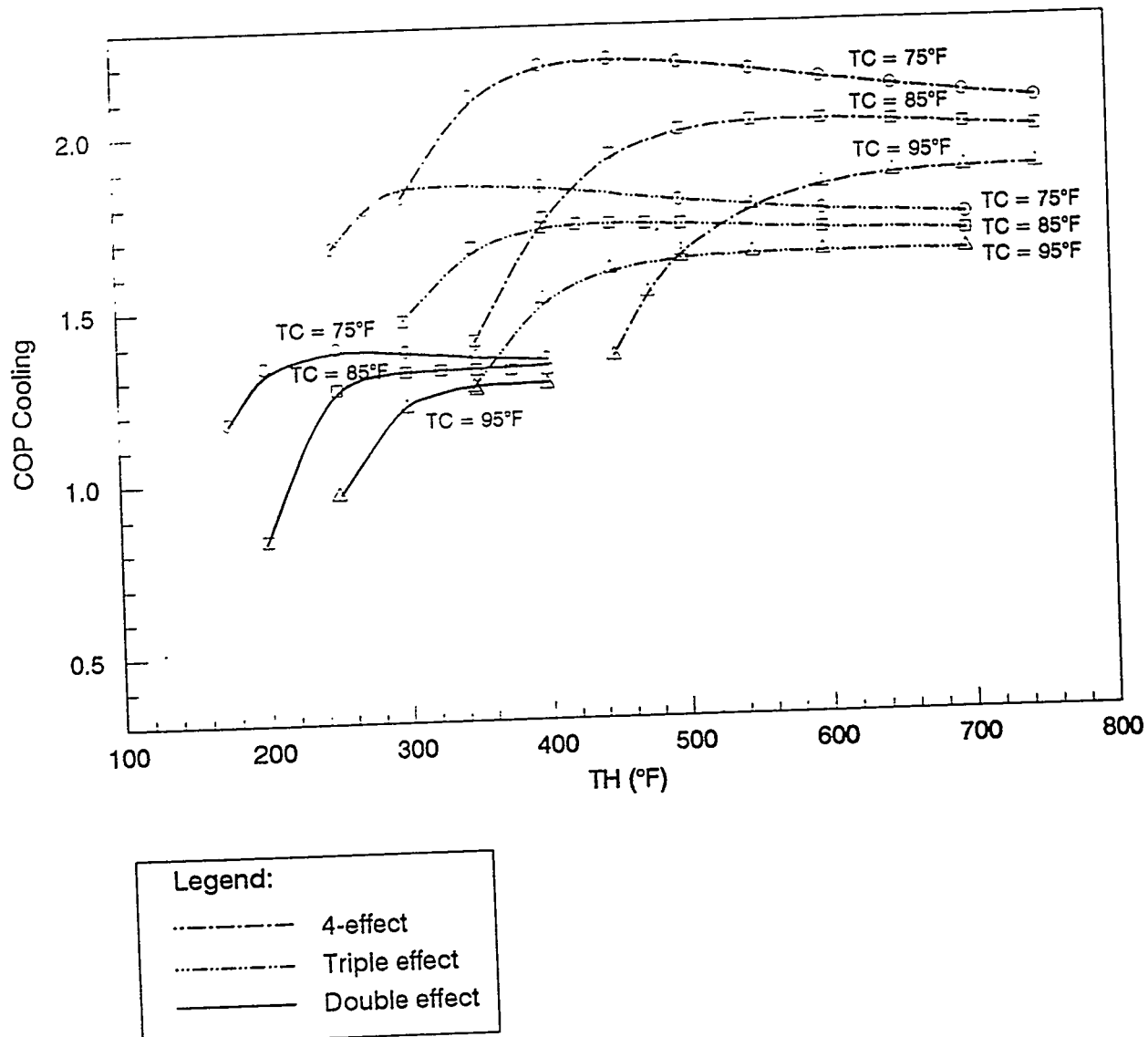


Figure 2.

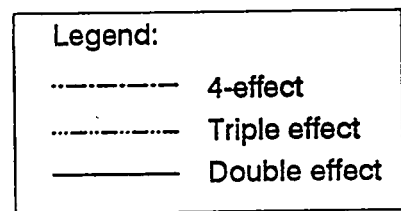
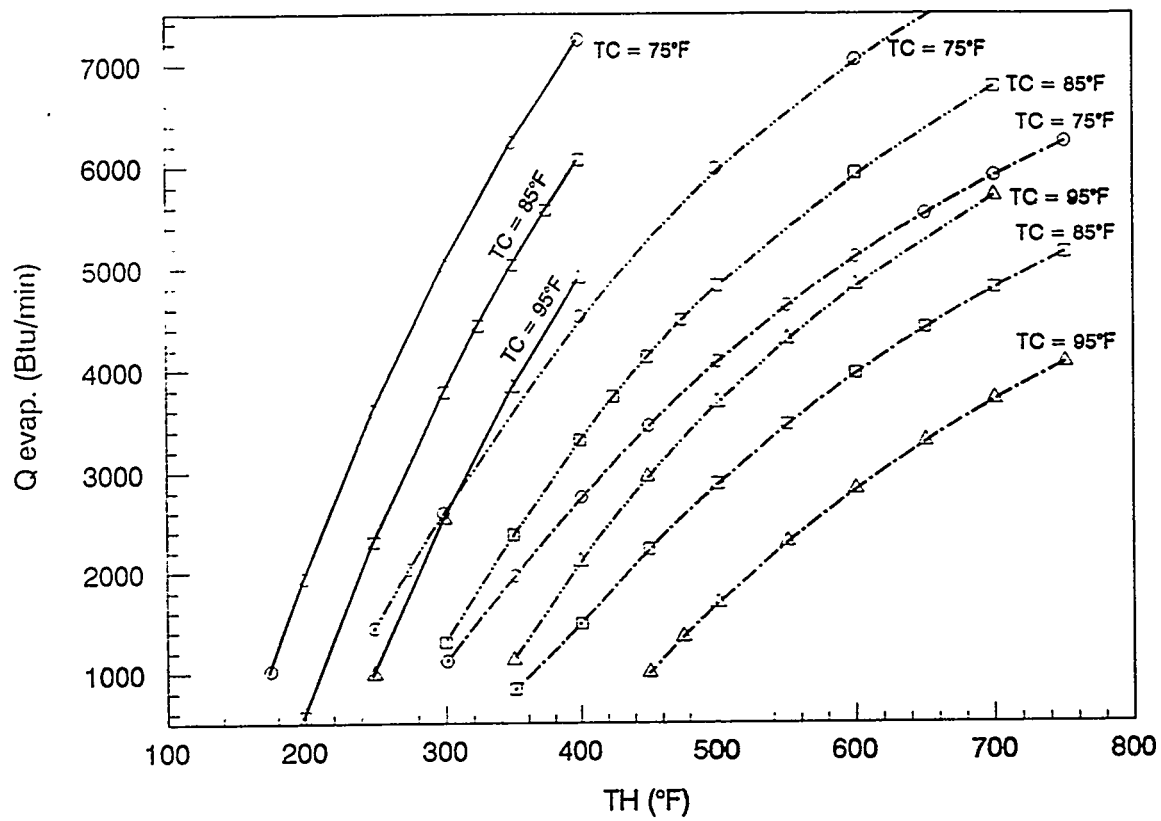


Figure 3.

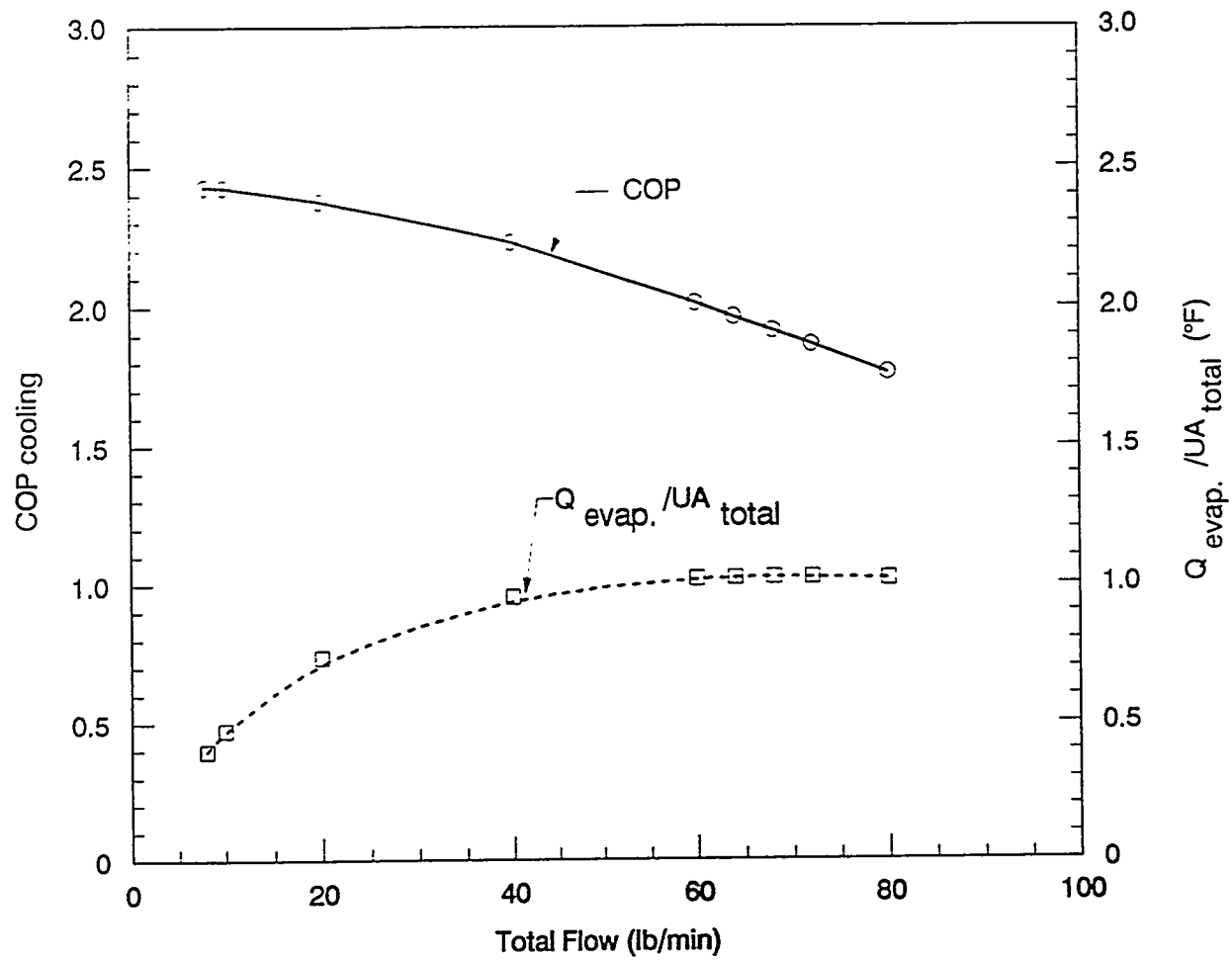


Figure 4.

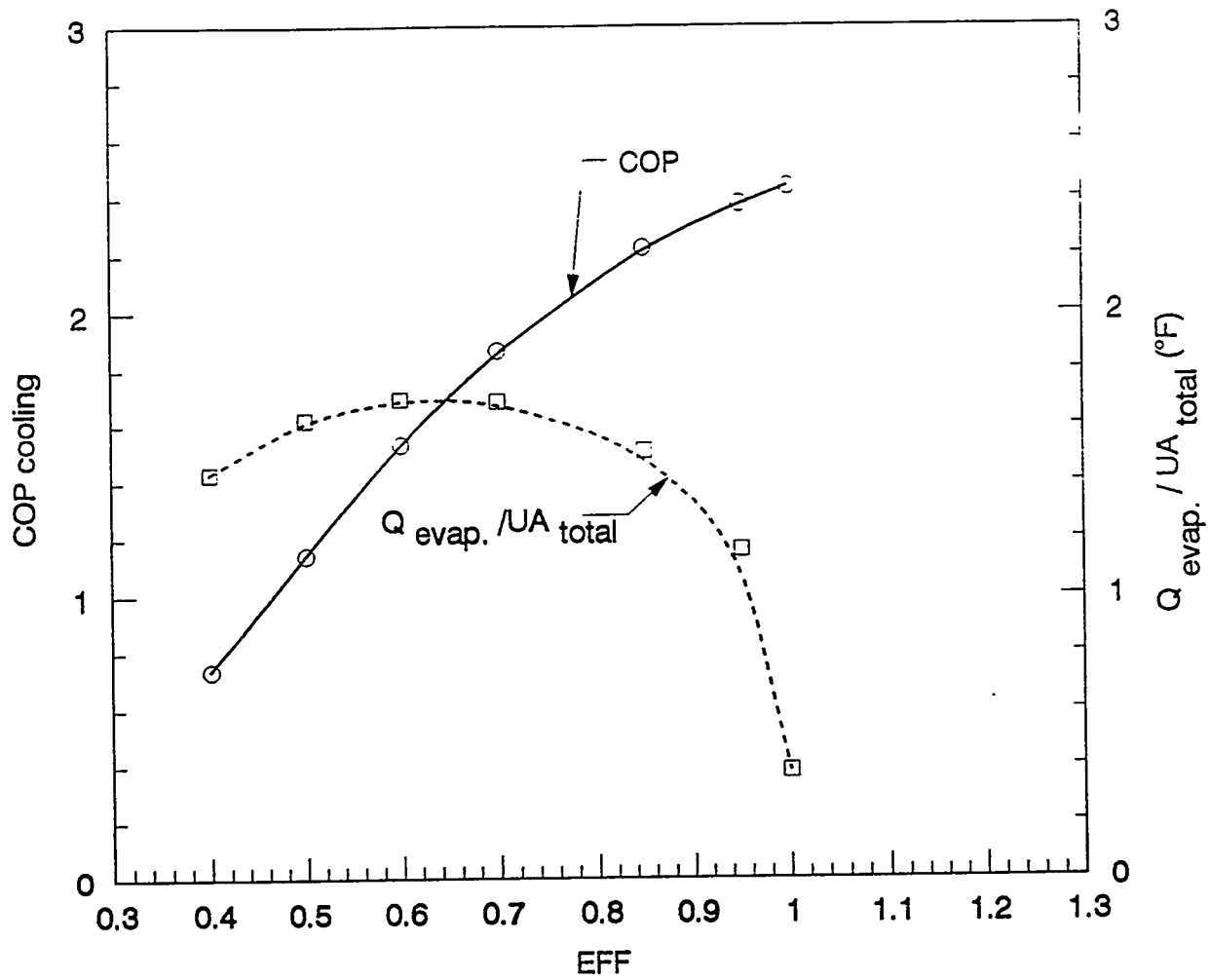


Figure 5.

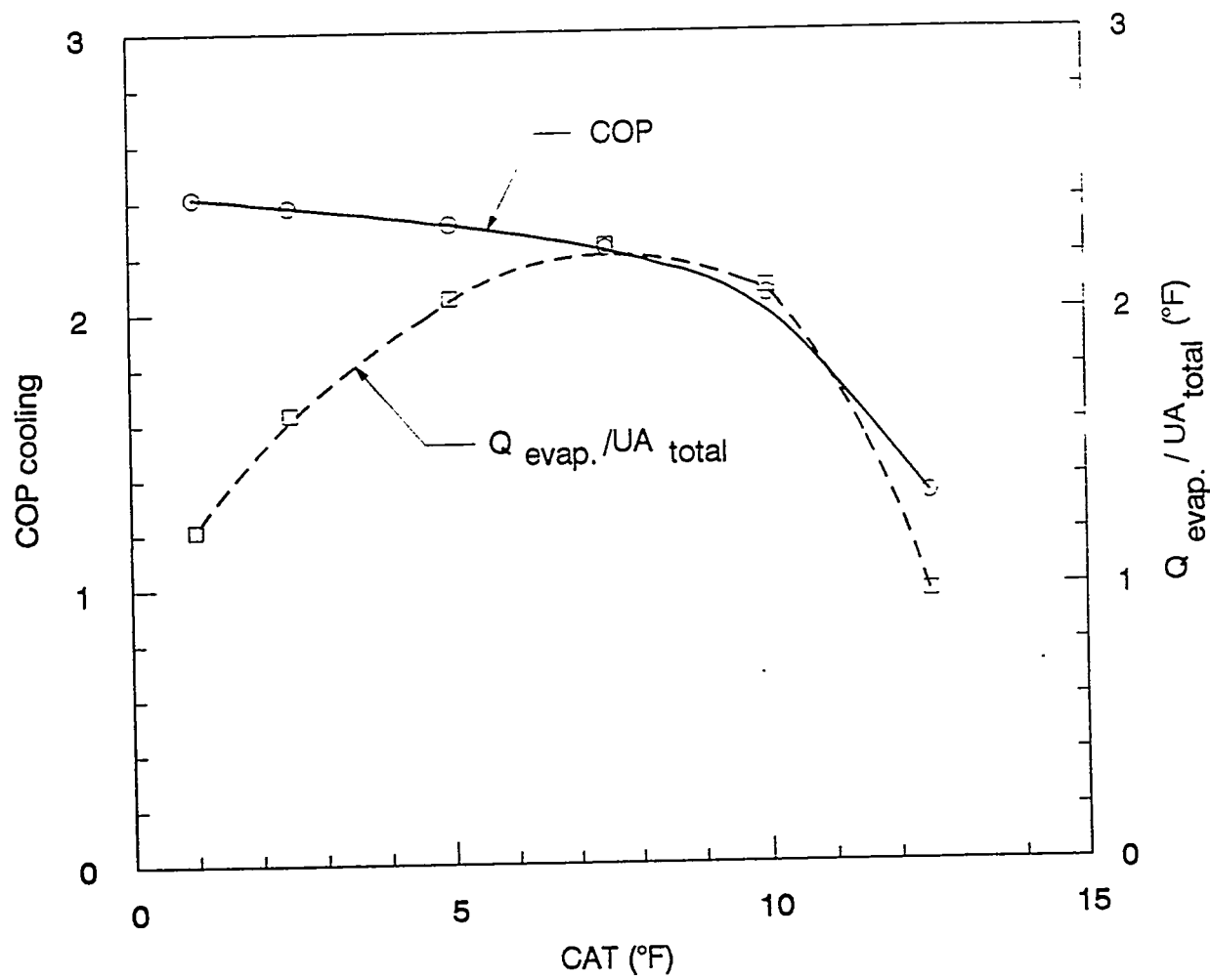
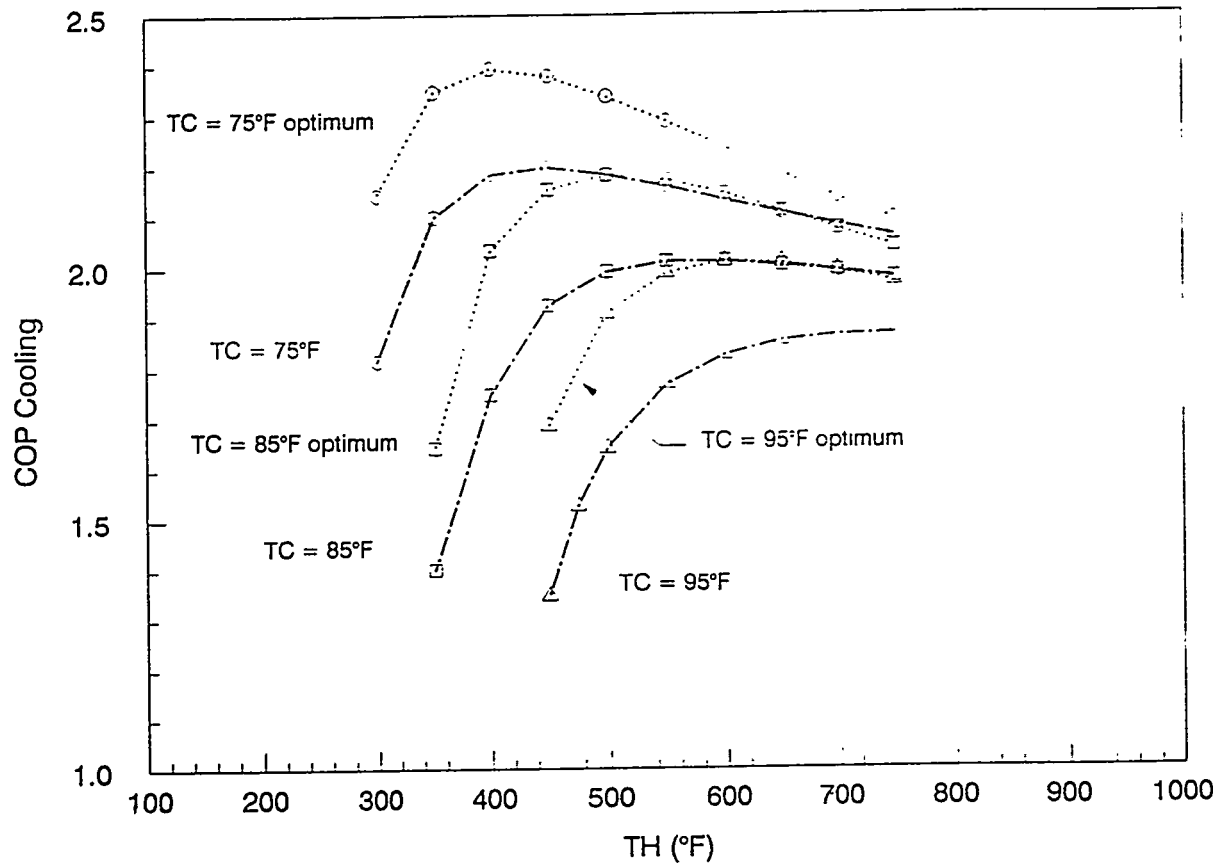


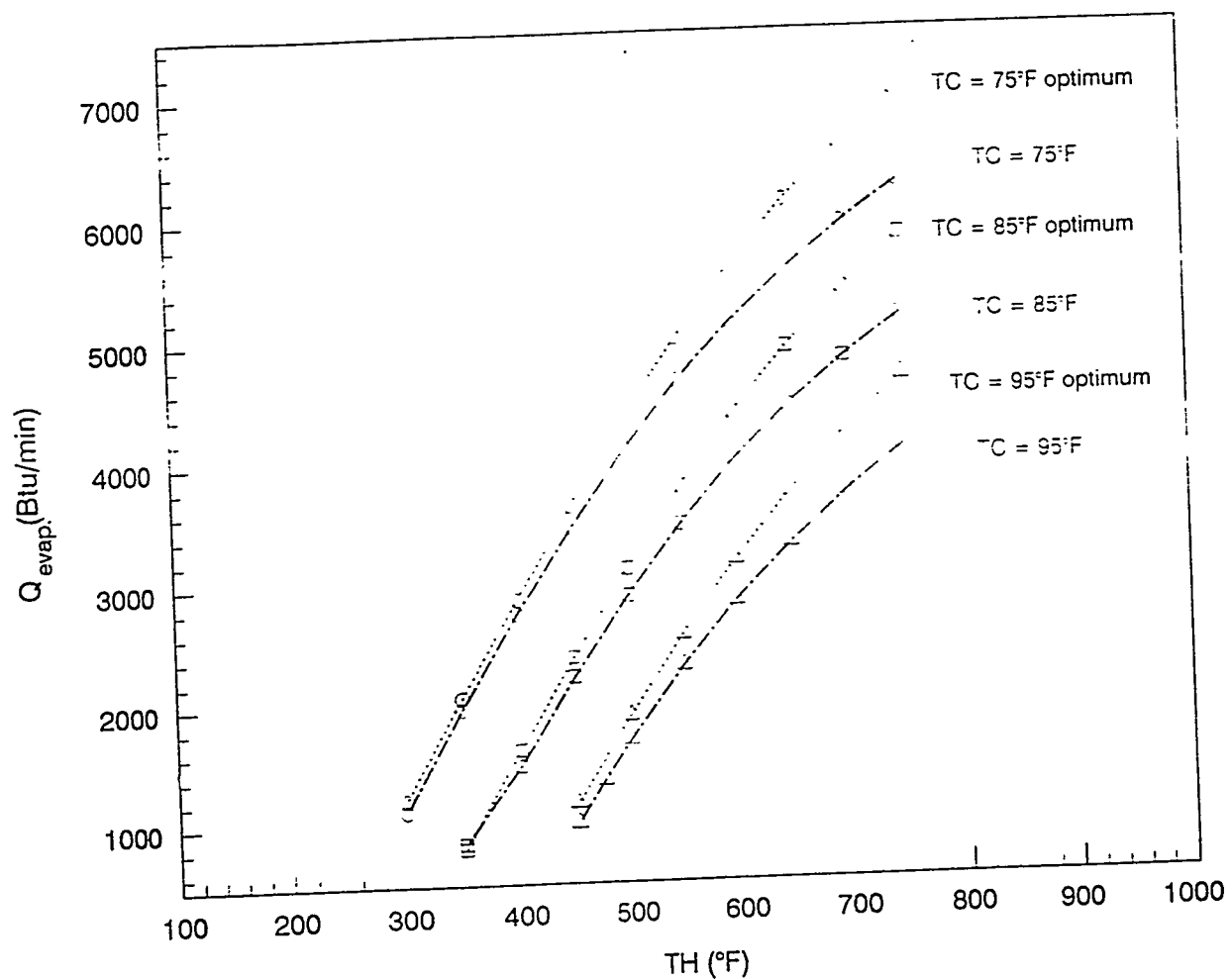
Figure 6.



**Legend:**

- ..... 4-effect, optimized size of components
- 4-effect, base case

Figure 7

**Legend:**

- ..... 4-effect, optimized size of components
- 4-effect, base case

Figure 8